Interactions and low-energy collisions between an alkali ion and an alkali atom of a different nucleus

2016 J. Phys. B: At. Mol. Opt. Phys. 49 105202

(http://iopscience.iop.org/0953-4075/49/10/105202)

IOP Publishing Journal of Physics B: Atomic, Molecular and Optical Physics
J. Phys. B: At. Mol. Opt. Phys. **49** (2016) 105202 (8pp) doi:10.1088/0953-4075/49/10/105202

Interactions and low-energy collisions between an alkali ion and an alkali atom of a different nucleus

Arpita Rakshit[1], Chedli Ghanmi[2,3], Hamid Berriche[2,4] and Bimalendu Deb[5]

[1] Sidhu Kanhu Birsa Polytechnic, Keshiary, Paschim Medinipur 721133, India
[2] Laboratory of Interfaces and Advanced Materials, Physics department, Faculty of Science, University of Monastir, 5019 Monastir, Tunisia
[3] Physics Department, Faculty of Science, King Khalid University, PO Box 9004, Abha, Saudi Arabia
[4] Mathematics and Natural Sciences Department, School of Arts and Sciences, American University of Ras Al Khaimah, Ras Al Khaimah, PO Box 10021, RAK, UAE
[5] Department of Materials Science, Raman Center for Atomic, Molecular and Optical Sciences, Indian Association for the Cultivation of Science, Jadavpur, Kolkata 700032, India

E-mail: msbd@iacs.res.in

Received 6 January 2016, revised 14 March 2016
Accepted for publication 5 April 2016
Published 5 May 2016

Abstract

We study theoretically interaction potentials and low-energy collisions between different alkali atoms and alkali ions. Specifically, we consider systems such as $X + Y^+$, where $X(Y^+)$ is either $Li(Cs^+)$ or $Cs(Li^+)$, $Na(Cs^+)$ or $Cs(Na^+)$ and $Li(Rb^+)$ or $Rb(Li^+)$. We calculate the molecular potentials of the ground and first two excited states of these three systems using a pseudopotential method and compare our results with those obtained by others. We derive ground-state scattering wave functions and analyze the cold collisional properties of these systems for a wide range of energies. We find that, in order to get convergent results for the total scattering cross sections for energies of the order 1 K, one needs to take into account at least 60 partial waves. The low-energy scattering properties calculated in this paper may serve as a precursor for experimental exploration of quantum collisions between an alkali atom and an alkali ion of a different nucleus.

Keywords: ion-atom cold collisions, potential curves, pseudopotential method

(Some figures may appear in colour only in the online journal)

1. Introduction

For more than three decades, there has been tremendous progress in the technology used for cooling and trapping of single-electron alkali atomic gases and some two-electron atomic gases. In parallel, developments in the technology of trapping and cooling of some ions, especially alkaline-earth cations, has led to new areas of research with trapped and cold ions. With recent experimental developments [1–16] using hybrid ion-atom traps [17], both atoms and ions can be confined simultaneously in a common space or an atom-trap can be merged with an ion-trap. These hybrid systems offer prospects for emulating solid-state physics with laser-generated periodic structures of ions [18] and for exploring the physics of ion-controlled Josephson junctions [19, 20] and Tonk–Girardeau gas with an ionic density 'bubble' [21].

At a fundamental level, these new hybrid devices facilitate laboratory investigations of ion-atom collisions in hitherto unexplored low-energy regimes—from milliKelvin down to microKelvin or sub-microKelvin temperature regimes. Ion-atom scattering at low energy is important for a number of physical systems, such as cold plasma, planetary atmospheres and interstellar clouds. Gaining insight into ion-atom interactions and scattering at ultralow energy down to the Wigner threshold law regime is important to understand charge transport [22] at low temperature, radiative association [2, 3, 23], ion-atom bound states [24], ion-atom photoassociation [25, 26], and many other related phenomena.

Several theoretical investigations [27–34] of atom-ion cold collisions have been carried out recently. It is proposed that controlled ion-atom cold collision can be utilized for quantum information processes [35, 36]. Several recent theoretical studies have focused on charge-transfer [37–39] and chemical reaction processes [40, 41] at ultralow energies between an alkaline-earth ion or Yb^+ and an alkali atom.

Ions are usually trapped by radio-frequency fields. The major hindrance to cooling trapped ions below milliKelvin temperatures stems from the trap-induced micro-motion of the ions, which seems to be indispensable for such ion traps. Therefore, it is difficult to achieve sub-microKelvin temperature for an ion-atom system in a hybrid trap. But, to explore fully quantum or Wigner threshold law regimes for ion-atom collisions, it is essential to reduce the temperature of ion-atom hybrid systems below one microKelvin. One way to overcome this difficulty is to devise new methods to trap and cool both ions and atoms in an optical trap. With the recent experimental demonstration of an optical trap for ions [42], the potential for experimental explorations of ultracold ion-atom collisions in the Wigner threshold regime appears to be promising.

In the context of the ion-atom cold collisions of our current interest, there are four main types of ion-atom systems: (1) an alkaline-earth ion interacting with an alkali-metal atom, (2) a rare-earth ion (such as Yb) interacting with an alkali-metal atom, (3) an alkali-metal ion interacting with an alkali atom of the same nucleus and (4) an alkali-metal ion interacting with an alkali atom of a different nucleus. In the first two types, both the ion and the atom have one valence electron in the outermost shell. In the third type, the ion has closed-shell structure while the atom has one valence electron in the outermost shell. Since both the ion and atom are of the same nucleus, there is a center of symmetry for the electronic wave function of the ion-atom pair. Because of this symmetry, resonant charge-transfer collision is possible in the third type. In the fourth type, the ion has a closed-shell structure while the atom has one valence electron in the outermost shell. Since the nuclei of the atom and the ion are different, there is no resonant charge-transfer collision in the fourth type, although non-resonant charge transfer is possible in all the types. For scattering in the ground-state potentials, non-resonant charge-transfer collision is suppressed in the ultralow energy regime ($<\mu$K).

We study cold collision in the fourth type of ion-atom systems here, although these systems are not straightforward to obtain experimentally. Normally, neutral alkali-metal atoms and alkaline-earth ions can be laser-cooled and trapped. However, there are some recent experimental studies showing different techniques [10, 11, 14, 15] for trapping and cooling of closed-shell alkali-metal ions. Our primary aim is to understand ground-state elastic scattering processes between such as an ion and an alkali atom of different nuclei at ultralow energy where the inelastic charge-transfer process can be ignored. A proper understanding of ground-state elastic scattering processes [33, 34] at low energy in an ion-atom system is important for exploring coherent control of ion-atom systems and the formation of ultracold molecular ions by radiative processes. Due to the absence of a resonance charge-transfer reaction, the fourth-type system is preferable for our purposes. However, there remains a finite possibility for inelastic collisions if the hyperfine structure of the neutral atom is taken in account. In our calculations we do not consider hyperfine interactions.

Let a cold alkali-metal ion $\mathbf{A}^+$ interact with a cold alkali-metal atom **B**. Suppose, the atomic mass of **B** is smaller than that of atom **A**. Then, for $\mathbf{AB}^+$ molecular system, the ground-state continuum asymptotically corresponds to the atom **B** (ns) in ^{2}S electronic state and the ion $\mathbf{A}^+$ (complete shell) in ^{1}S electronic state. In the separated atom limit, the first excited molecular potential asymptotically goes as the atom **A** (ns) in ^{2}S electronic state and alkali ion $\mathbf{B}^+$ (complete shell) in ^{1}S electronic state while the second electronic excited potential corresponds to **B** (np) in ^{2}P electronic state and alkali ion $\mathbf{A}^+$ (complete shell) in ^{1}S electronic state.

We investigate cold collisions over a wide range of energies in three different alkali atom–alkali ion systems in the ground molecular potentials. The colliding atom-ion pairs we consider are: (i) $Cs^+ + Li$, (ii) $Cs^+ + Na$, and (iii) $Rb^+ + Li$. Since at ultralow energy, the charge-transfer reaction is highly suppressed in these systems, we study elastic scattering only. To calculate scattering wave functions, we need the data for Born–Oppenheimer adiabatic potentials of the systems. In the long range where the separation $r > 20\ a_0$ (a_0 is the Bohr radius), the potential is given by the sum of the dispersion terms, which in the leading order goes as $1/r^4$. We obtain short-range potentials by using a pseudopotential method. The short-range part is combined smoothly with the long-range part to obtain the potential for the entire range. We then solve the time-independent Schrödinger equation for these potentials with scattering boundary conditions by using the Numerov–Cooley [43] algorithm. We present detailed results of scattering cross sections for these three systems for energies ranging from 0.01 microKelvin (μK) to 1 Kelvin (K). However, the low-energy regime of our interest ranges from sub-μKto 1 milliKelvin (mK). Here we choose to use Kelvin as the unit of energy to readily convey information about how cold the system should be to explore such collision physics. Normally the results of atomic collisions are expressed in atomic units (a.u.). Note that 1 a.u. of energy corresponds to 3.1577465×10^5 K or 27.21138386 electron-volts (ev).

2. Interactions and molecular properties

Under the Born–Oppenheimer approximation, we compute the adiabatic potential energy curves of the $1^2\Sigma^+$, $2^2\Sigma^+$ and $3^2\Sigma^+$ electronic states of the three ionic molecules $(LiRb)^+$, $(LiCs)^+$ and $(NaCs)^+$ using the pseudopotential method proposed by Barthelat and Durand [44] in its semi-local form and used in many previous works [45–49]. The interaction potentials between different alkali-metal ions and an alkali-metal atom were calculated by Valance [50] in 1978 by using pseudopotential method. Here we briefly describe spectroscopic constants and interaction potentials of the three

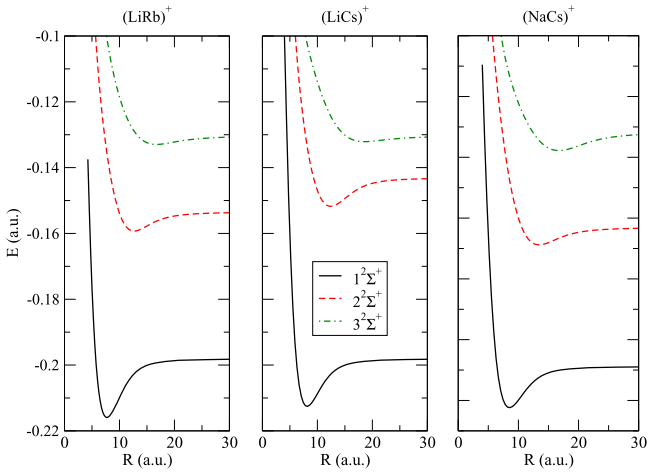

Figure 1. Adiabatic potential curves for $(LiRb)^+$, $(LiCs)^+$ and $(NaCs)^+$.

considered atom-ion systems, and the pseudopotential method used to obtain these molecular properties. Our final goal is to calculate the cold collisional properties of these systems using these potentials, as described in the next section.

2.1. Adiabatic potentials

For the three ionic systems $(LiRb)^+$, $(LiCs)^+$ and $(NaCs)^+$, the potential energy curves of the 1-$3^2\Sigma^+$ electronic states, are built from an *ab initio* calculation for the internuclear distances ranging from 3 to 200 a_0 (a_0 is Bohr radius) as discussed in sub-section 2.2. These states dissociate respectively, into Li(2 s and 2p) + Rb^+ and Rb(5s) + Li^+, Li(2 s and 2p) + Cs^+ and Cs(6s) + Li^+, and Na(3 s and 3p) + Cs^+ and Cs(6s) + Na^+. They are displayed in figure 1(a) for $LiRb^+$, 1(b) $LiCs^+$ and 1(c) for $NaCs^+$. In the long-range part beyond 200 a_0, the potential is given by the sum of the dispersion terms The short-range part ($\leqslant 20\, a_0$) of *ab initio* potential is combined smoothly with the long-range part by interpolation to obtain the potential for entire range extending to several thousand a_0. For the three ionic systems, we remark that the ground state has the deepest well compared to the $2^2\Sigma^+$ and $3^2\Sigma^+$ excited states. Their dissociation energies are of the order of several 1000 cm^{-1}. Their equilibrium positions lie at separations that are relatively larger than those of typical neutral alkali-alkali diatomic molecules.

The long-range potential is given by the expression

$$V(r) = -\frac{1}{2}\left(\frac{C_4}{r^4} + \frac{C_6}{r^6} + \cdots\right) \tag{1}$$

where C_4, C_6 correspond to dipole, quadrupole polarisabilities of concerned atom. Hence, the long-range interaction is governed predominately by polarisation interaction. Dipole polarisabilities for Na (3s) and Li (2s) are 162 a.u. and 164.14 a.u., respectively. One can define a characteristic length scale of the long-range potentials by $\beta = \sqrt{2\mu C_4/\hbar^2}$. The values of β for the collision of Li–Cs^+ pair and Na—Cs^+ pair are 1411.5 a.u. and 2405.8 a.u., respectively.

For the ground state $1^2\Sigma^+$ the well depth and the equilibrium position are 2979 cm^{-1} and 8.51 a.u., respectively, for $(NaCs)^+$ while those for $(LiCs)^+$ are 3176 cm^{-1} and 8.12 a.u., respectively. Reduced masses for $(NaCs)^+$ and $(LiCs)^+$ (for ^{7}Li isotope) are taken as 19.5995 a.u. and 6.6642 a.u., respectively. For both ^{6}Li-Rb^+ and ^{6}Li-Rb^+ isotopes, we used the reduced masses 5.6171 and 6.4805 a.u. respectively.

2.2. Pseudopotential method: results and discussions

The use of the pseudopotential method for each $(XY)^+$ ionic molecule ($LiRb^+$, $LiCs^+$ and $NaCs^+$) reduces the number of active electrons to only one. We have used a core polarization potential V_{CPP} for the simulation of the interaction between the polarizable X^+ and Y^+ cores with the valence electron. This core polarization potential is used according to the formulation of Müller *et al* [51], and is given by

$$V_{CPP} = -\frac{1}{2}\Sigma_\lambda \alpha_\lambda \vec{f}_\lambda \cdot \vec{f}_\lambda \tag{2}$$

where α_λ and $\vec{f}_\lambda$ are respectively the dipole polarizability of the core λ, and the electric field produced by valence electrons and all other cores on the core λ. The electric field $\vec{f}_\lambda$ is defined as:

$$\vec{f}_\lambda = \Sigma_i \frac{\vec{r}_{i\lambda}}{r_i^3} F(\vec{r}_{i\lambda}, \rho_\lambda) - \Sigma_{\lambda' \neq \lambda} \frac{\vec{R}_{\lambda',\lambda}}{R_{\lambda',\lambda}^3} Z_\lambda \tag{3}$$

where $\vec{r}_{i\lambda}$ and $\vec{R}_{\lambda,\lambda}$ are respectively the core-electron vector and the core–core vector.

Based on the formulation of Foucrault *et al* [52] the cut-off function $F(\vec{r}_{i\lambda}, \rho_\lambda)$ is a function of the quantum number l. In this formulation, the interactions of valence electrons of different spatial symmetry with core electrons are considered in a different way. The used cut-off radii of the lowest valence s, p, d and f one electron for the Li, Na, Rb and Cs atoms are taken from [45, 47–49]. The extended Gaussian-type basis sets used for Li, Na, Rb and Cs atoms are respectively (9s8p5d1f/8s6p3d1f) [48], (7s6p5d3f/6s5p4d2f) [48], (7s4p5d1f/6s4p4d1f) [53] and (7s4p5d1f/6s4p4d1f) [46]. The used core polarizabilities of Li^+, Na^+, Rb^+ and Cs^+ cores, which are equal respectively 0.1915 a_0^3, 0.993 a_0^3, 9.245 a_0^3 and 15.117 a_0^3 are taken from [51]. By using the pseudopotential technique, each molecule is reduced to only one valence electron interacting with two cores. Within the Born–Oppenheimer approximation, a self-consistent field (SCF) calculation provides us with accurate potential energy curves and dipole functions.

2.3. Spectroscopic constants

The spectroscopic constants (R_e, D_e, T_e, ω_e, $\omega_e\chi_e$, B_e) of the 1-$3^2\Sigma^+$ electronic states are presented in tables 1–4 for $(LiRb)^+$, $(LiCs)^+$ and $(NaCs)^+$, respectively. To the best of our knowledge, no experimental data has been found for these systems. We compare our spectroscopic constants only with the available theoretical results. Table 1 presents the spectroscopic constants of $(LiRb)^+$ compared with the other theoretical works [54–57]. As it seems from table 1, there is a good agreement between the available theoretical works [54–57] and our *ab initio* study. Azizi *et al* [57] reported the

Table 1. A comparison of the spectroscopic constants for the ground ($X^2\Sigma^+$) and the first and second excited ($2^2\Sigma^+$ and $3^2\Sigma^+$) electronic states of $(LiRb)^+$ molecular ion with the available works.

State	R_e(a.u.)	D_e(cm^{-1})	T_e, (cm^{-1})	ω_e(cm^{-1})	$\omega_e\chi_e$(cm^{-1})	B_e(cm^{-1})	References
$X^2\Sigma^+$	7.70	3912		137.56	1.67	0.158098	This work
		3705					[54]
	7.50						[55]
	7.60	3432					[56]
	7.54	4193		139.65			[57]
$2^2\Sigma^+$	12.67	1270	12438	63.73	0.51	0.058456	This work
	12.60	1306		63.00			[57]
$3^2\Sigma^+$	16.66	617	18200	35.73	1.55	0.033769	This work

Table 2. A comparison of the spectroscopic constants for the ground ($X^2\Sigma^+$) and the first and second excited ($2^2\Sigma^+$ and $3^2\Sigma^+$) electronic states of $(LiCs)^+$ molecular ion with the work of Khelifi *et al* [57].

State	R_e(a.u.)	D_e(cm^{-1})	T_e,(cm^{-1})	ω_e(cm^{-1})	$\omega_e\chi_e$(cm^{-1})	B_e(cm^{-1})	References
$1^2\Sigma^+$	8.12	3176	0	124.46	1.08	0.138337	This work
	7.19	3543					[58]
$2^2\Sigma^+$	12.42	1911	13343	68.69	0.63	0.059126	This work
	12.37	2022	19553				[58]
$3^2\Sigma^+$	18.53	422	17660	28.07	1.29	0.026570	This work
	18.38	409	20849				[58]

Table 3. A comparison of the spectroscopic constants for the ground ($X^2\Sigma^+$) and the first and second excited ($2^2\Sigma^+$ and $3^2\Sigma^+$) electronic states of $(NaCs)^+$ molecular ion with the work of Valance [49].

State	R_e(a.u.)	D_e(cm^{-1})	T_e,(cm^{-1})	ω_e(cm^{-1})	$\omega_e\chi_e$(cm^{-1})	B_e(cm^{-1})	References
$1^2\Sigma^+$	8.51	2979	0	68.17	0.32	0.042418	This work
	7.60	3388					[50]
$2^2\Sigma^+$	13.45	1262	11758	33.98	0.30	0.016977	This work
	14.20	774					[50]
$3^2\Sigma^+$	16.77	1393	18553	26.20	1.69	0.010920	This work
	15.00	732					[50]

spectroscopic constants for many ionic alkali dimers, but only for the ground and the first excited states. In their study, they used a similar formalism as used in our work. We remark that our ground-state equilibrium distance (R_e) presents a satisfying agreement as well as the well depth (D_e) with the work of Azizi *et al* [57]. We found for (R_e) and (D_e), respectively, 7.70 a.u. and 3912 cm^{-1} and they found 7.54 a.u. and 4193 cm^{-1}. The difference between the results of Azizi *et al* [57] and our values are about 2.12% and 6.70% for R_e and D_e, respectively. The same agreement is observed between our harmonicity frequency (ω_e) and that of Azizi *et al* [57]. The difference between the two values is 2.09 cm^{-1}, which represents a difference of 1.49%. There is also a very good agreement between our equilibrium distance and that of Patil *et al* [56] ($R_e = 7.60$ a.u.), in contrast to their well depth [56], which is underestimated ($D_e = 3432$ cm^{-1}). For the first excited state, Azizi *et al* [57] reported the spectroscopic constants $R_e = 12.60$ a.u., $D_e = 1306$ cm^{-1} and $\omega_e = 63.00$ cm^{-1} to be compared with our values of, respectively, 12.67 a.u., 1270 and 63.73 cm^{-1}. The differences in percentages between the values obtained by Azizi *et al* [57] and our results are 0.55%, 2.75% and 1.14% for R_e, D_e and ω_e, respectively.

The spectroscopic constants of $(LiCs)^+$ and $(NaCs)^+$, are presented respectively in tables 4–4 and compared with the available theoretical results [50, 58]. To the best of our knowledge there is no experimental data for these ionic molecules. For the $(LiCs)^+$ ionic molecule, we compare our results only with the theoretical work of Khelifi *et al* [58] where they used a similar method as used in our work. They reported for the ground state $1^2\Sigma^+$ the spectroscopic constants $R_e = 7.91$ a.u. and $D_e = 3543$ cm^{-1} to be compared with our values of, respectively, $R_e = 8.12$ a.u. and $D_e = 3176$ cm^{-1}. A rather good agreement is observed for the equilibrium distance, however their potential is much deeper. Reasonably good agreement between our spectroscopic constant and those of Khelifi *et al* [58] is observed for the $2^2\Sigma^+$ and $3^2\Sigma^+$ states. The difference between Khelifi *et al*'s spectroscopic constants and our results are found to be 2.58% and 10.35% for R_e and D_e, respectively. For the ground state of the $(NaCs)^+$ ionic molecule, there is a good agreement between our well depth, as well as the equilibrium distance with the theoretical results

of Valance [50]. We found a well depth of 2979 cm^{-1} located at 8.51 a.u., while Valance [50] found 3388 cm^{-1} located at 7.60 a.u. The difference in percentages between Valance's data and our values are 12.07% and 11.97% for R_e and D_e, respectively. In contrast to the ground state, where the agreement between our work and those of Valance [50] is good, there is disagreement for the $2^2\Sigma^+$ and $3^2\Sigma^+$ states. The two states exhibit small potential wells in Valance's work equal, respectively, to 774 and 732 cm^{-1}; while in our work we have found significantly higher well depths of 1262 and 1393 cm^{-1}, respectively. Our well depth for the $2^2\Sigma^+$ and $3^2\Sigma^+$ states are of 63.04% and 90.30% larger than those of Valance [50].

The large discrepancies between the Valences results and our values can be explained by two reason. First, Valence used the Hellmann-type model where the Hamiltonian is written in terms of one valence electron interacting with closed shell cores. Therefore, the core-core interaction potentials were neglected. This is certainly true for large interatomic distances but it is not accurate enough for small separations. Valence considered this shortcoming as not relevant to the charge exchange collision process they studied using the interaction potential where only intermediate and long-range distances are required. Although, without considering the core-core interaction one can get correct asymptotic limits, at intermediate distance this will affect the accuracy of the equilibrium distance and well depth. Second, the core-valence interactions were considered in our work using a formulation where, for each atom, the core polarization effects are described by an effective potential as described previously. The latter is modified by an *l*- dependent cut-off function *F* to take into account the orbital symmetries. In the case of Valence, the Hellmann pseudopotential is not '*l*'-dependent and the parameters are optimized to obtain the two first experimental energy levels. Similarly, in the the absence of the core–core interaction, Valence considered that this lack of '*l*' dependence as not being crucial for the charge-exchange collision. In our approach, in addition to the use of an *l*-dependent pseudopotential, the parameters were optimized to reproduce with high accuracy the ionization potential and the experimental energy levels of many alkali excited states. Moreover, in our study, the interatomic separation grid is more extensive as *R* varies from 3 to 200 a.u. with a distance step of 0.1 a.u, but Valence limited his calculation for internuclear distances ranging from 5 a.u. to 25 a.u. It is important to note that the calculation time in our calculation is reduced enormously due to the use of the pseudopotential approach that leads these ionic molecules to one-electron systems. Calculations are performed on a desktop Pentium IV Acer computer where the time for one single distance is about 32 s.

3. Elastic collisions: results and discussions

Here we present results on elastic collisions of the discussed ion-atom systems by using FORTRAN code [59] using the well-known Numerov–Cooley algorithm [43]. This algorithm provides an efficient technique for numerically solving a second-order differential equation. It uses a three-point recursion relation to calculate the first-order derivative and makes use of the exact second-order derivative provided by the equation itself. To solve the time-independent Schrödinger equation as a scattering problem, one has to propagate the Numerov–Cooley code from an initially small internuclear separation *r* to asymptotically large *r* where the wave function corresponds to the state of a free particle and so behaves sinusoidally. The scattering *S*-matrix is then deduced by matching the asymptotic solution with the standard scattering boundary conditions. The correctness of the calculations is ensured by the unitarity of the *S*-matrix. The lower the energy the larger the asymptotic boundary is. To initiate the propagation of the code from $r \simeq 0$ position, one has to initially set the values of the wave functions at two initial positions, then the code calculates the wave function for the third position, and then taking the the values of the wave functions for the second and third position it calculates the wave function for the fourth position, and the process continues until the asymptotic boundary is reached. The initial boundary conditions are set by expanding the interaction potential for small *r* and solving the Schrödinger equation analytically for the $r \to 0$ limit. A good measure for the asymptotic scattering boundary (large *r*) can be found by setting the condition that the effective potential $V_{\rm eff} = -C_6/r^6 + (\hbar^2/2\mu)\ell(\ell+1)/r^2$ for large *r* becomes much less than the collision energy *E* (at least one tenth of *E*).

We use the interaction potentials calculated above as input data. In particular, we focus on low-energy collisions. Using the well-known expansion of a continuum state in terms of partial waves, the wave function ψ_ℓ (k r) for the ℓth partial wave is given by

$$\left[\frac{\mathrm{d}^2}{\mathrm{d}r^2} + k^2 - \frac{2\mu}{\hbar^2}V(r) - \frac{\ell(\ell+1)}{r^2}\right]\psi_\ell(kr) = 0 \qquad (4)$$

subject to the standard scattering boundary condition

$$\psi_\ell(kr) \sim \sin[kr - \ell\pi/2 + \eta_l] \qquad (5)$$

Here *r* denotes the ion-atom separation, the wave number *k* is related to the collision energy *E* by $E = \hbar^2k^2/2\mu$ and μ stands for the reduced mass of the ion-atom pair. The total elastic scattering cross section is given by

$$\sigma_{\rm el} = \frac{4\pi}{k^2}\sum_{\ell=0}^{\infty}(2\ell+1)\sin^2(\eta_\ell). \qquad (6)$$

To know the relevant energy regimes where *s*- *p*- and *d*-wave collisions are important, we have plotted in figure 2 the centrifugal energies for first three partial waves ($\ell = 0$, 1 and 2) against ion-atom separations for ground state $1^2\Sigma^+$ of $(NaCs)^+$ and $(LiCs)^+$, respectively. For the *d*-wave, the values of the centrifugal barrier are about 0.007 mK for $(NaCs)^+$ and about 0.06 mK for $(LiCs)^+$. These values indicate that the potential energy barriers for low-lying higher partial waves are very low for atom-ion systems allowing tunneling of the wave function towards the inner region of the barriers. Unlike atom–atom systems at low energy, a number of partial waves can significantly contribute to the ion-atom

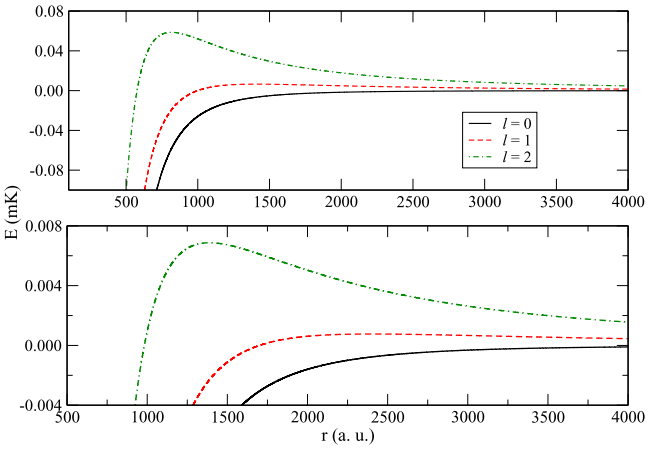

Figure 2. In the upper panel, the centrifugal energies in units of milliKelvin (mK) for *s*- (black, solid), *p*- (red, dashed) and *d*- (green, dashed-dotted) partial waves are plotted against atom-ion separation for $l^2\Sigma^+$ state of $(LiCs)^+$. The lower panel shows the same for $(NaCs)^+$.

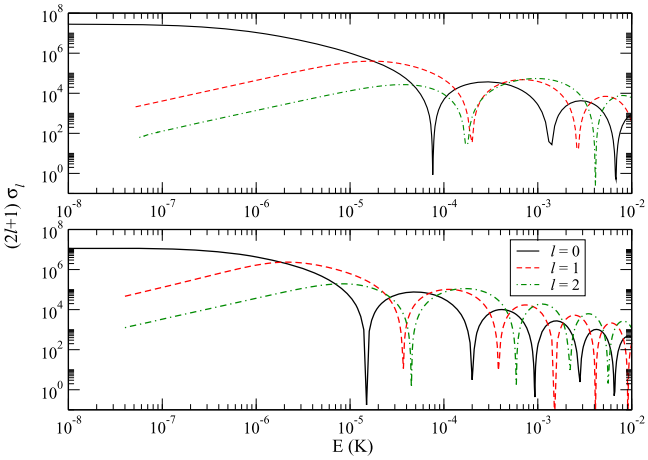

Figure 3. *s*- *p*- and *d*-wave scattering cross sections in atomic units (a.u.) or in units of a_0^2 (a_0 is Bohr radius) are plotted against collision energy E in Kelvin (K) for $l^2\Sigma^+$ state of $(LiCs)^+$ and $(NaCs)^+$ in upper and lower panel, respectively.

scattering cross section at low energy. We find that in order to get convergent results at milli- and microKelvin regimes, the numerical calculation of the scattering wave function needs to be extended to at least 10000 a_0 and 20000 a_0, respectively.

In figure 3, the partial-wave cross sections for ground $1^2\Sigma^+$ state collisions are plotted against collision energy E in K for $(NaCs)^+$ and $(LiCs)^+$. As $k \to 0$, *s*-wave cross section becomes independent of energy while *p*- and *d*-wave cross sections vary in accordance with Wigner threshold laws. According to Wigner threshold laws, as $k \to 0$, the phase shift for ℓth partial-wave $\eta_l \sim k^{2\ell+1}$ if $\ell \leqslant (n-3)/2$, otherwise $\eta_l \sim k^{n-2}$ for a long-range potential behaving as $1/r^n$. Since Born–Oppenheimer ion-atom potential goes as $1/r^4$ in the asymptotic limit, as $k \to 0$, *s*-wave scattering cross section becomes independent of energy while all other higher partial-wave cross sections go as $\sim k^2$. As energy increases beyond the Wigner threshold law regime, the *s*-wave cross section exhibits a minimum at a low energy which may be related to

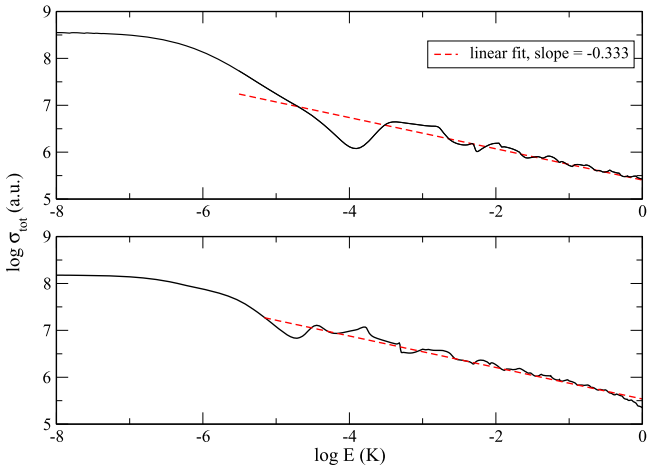

Figure 4. Logarithm of total scattering cross section in a.u. as a function of logarithm of energy E in K for electronic ground-state $l^2\Sigma^+$ of $(LiCs)^+$ and $(NaCs)^+$ are plotted in upper and lower panel, respectively.

the Ramsauer–Townsend effect. It can be noticed from figure 3 that at Ramsauer minimum of *s*-wave scattering, the *p*- and *d*-wave elastic cross sections are finite. This means that one can explore *p*- or *d*-wave interactions of ion-atom systems at the minimum position that occurs at a relatively low energy (μ- and milliKelvin regime).

In the Wigner threshold regime, hetero-nuclear ion-atom collisions are dominated by elastic scattering processes since the charge-transfer reactions are highly suppressed in this energy regime. Furthermore, resonant charge-transfer collisions do not arise in collisions of an ion with an atom of different nucleus.

It is worthwhile to compare the elastic scattering results of a hetero-nuclear alkali ion-atom system to those of a homo-nuclear alkali atom-ion system $Na+Na^+$ [22]. By comparing our results in figure 3 with figures 2 and 3 of [22], we notice that the elastic scattering cross sections of both homo- and hetero-nuclear ion-atom systems at ultralow energies are comparable and primarily governed by Winger threshold laws. However, unlike hetero-nuclear systems, the resonant charge-transfer cross section in homo-nuclear $Na+Na^+$ is also of the same order as that of elastic one at ultralow energies. Resonant charge-exchange cold collisions between Yb and Yb^+ are experimentally observed and found to be a dominant process in this homo-nuclear system [1].

In figure 4, we have plotted logarithm of total elastic scattering cross sections (σ_{tot}) expressed in a.u. as a function of logarithm of E in K for ground-state collisions between Li and Cs^+ and between Na and Cs^+, respectively. For both $(LiCs)^+$ and $(NaCs)^+$, to calculate σ_{tot}, we require more than 60 partial waves to get converging results for energies greater than 1 mK. This is because, as the collision energy increases, more and more partial waves start to contribute to σ_{tot}. In order for a particular partial wave ℓ to contribute appreciably at a given energy E, the centrifugal barrier height corresponding to this partial wave should not be too high compared to the energy. An estimate of the minimum number of partial

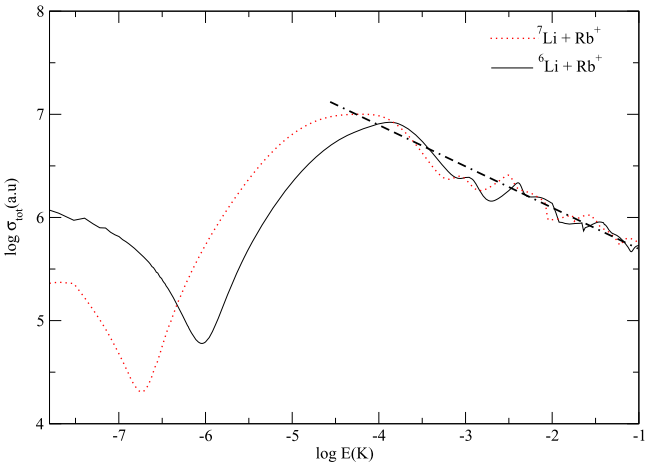

Figure 5. Same as in figure 4 but for Li + ^{87}Rb$^+$ ($1^2\Sigma^+$) collision. The black solid line and red dotted lines are for ^{6}Li and ^{7}Li, respectively. Black dashed lines represent linear fit to both the curves for energies greater than 10^{-6} K. Both cases follow one-third law and the intercepts are found to be 3.587 and 3.606 in a.u. for ^{6}Li and ^{7}Li, respectively; where as the theoretically calculated values are 3.3269 and 3.3476 in a.u., respectively.

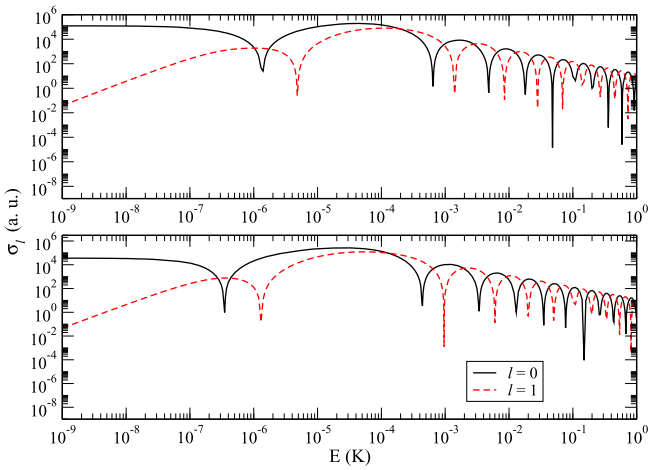

Figure 6. Partial wave cross sections for ^{6}Li + Rb$^+$ ($1^2\Sigma^+$) and ^{7}Li + Rb$^+$ ($1^2\Sigma^+$) collision are plotted as a function of E (in K) for $\ell = 0$ (solid) and $\ell = 1$ (dashed) in upper and lower panel, respectively.

waves required for obtaining convergent results may be made by taking the height of the centrifugal barrier to be higher than the energy by one order of magnitude. In this context, it is worth mentioning that the centrifugal barrier height for a partial wave of an ion-atom system is usually much lower than the corresponding height of atom–atom system, therefore larger number of partial waves contribute to $\sigma_{\rm tot}$ in case of an ion-atom system. In the large energy limit, the cross section behaves as

$$\sigma_{\rm tot} \sim \pi \left(\frac{\mu C_4^2}{\hbar^2}\right)^{\frac{1}{3}} \left(1 + \frac{\pi^2}{16}\right) E^{-\frac{1}{3}} \qquad (7)$$

Thus, in the large energy regime the slope of the logarithm of $\sigma_{\rm tot}$ as a function of $\log E$ is a straight line obeying the equation $\sigma_{\rm tot}(E) = -(1/3)E + c_E$ where the slope of the line is $-1/3$ and the intercept of the line on the energy axis is solely determined by the C_4 coefficient of long-range part of the potential, or equivalently by the characteristic length scale β of the potentials or the polarizability of the neutral atom interacting with the ion. As shown in figure 4, we have numerically verified this $E^{-1/3}$ law for both Li-Cs$^+$ and Na-Cs$^+$ systems. The linear fit to the the plot of numerically calculated $\sigma_{\rm tot}$ against the large energy regime shows that the value of the slope is quite close to the actual value of $1/3$. Since the dipole polarizability of Li and Na is not much different, one can expect that for both Li-Cs$^+$ and Na-Cs$^+$ systems, the energy dependence of $\sigma_{\rm tot}$ at large energy should be similar. In fact, figure 4 shows that for energies much greater 1 μK, both systems exhibit similar asymptotic energy dependence.

Finally, we consider the collision of ^{85}Rb$^+$ with the two isotopes of the Li atom, namely, ^{6}Li and ^{7}Li, and the results are shown in figures 5 and 6. The purpose here is to investigate the isotopic effects of Li on low-energy collisions with a ^{85}Rb$^+$ ion. In figure 5 we have plotted the logarithm (to the base of 10) of $\sigma_{\rm tot}$ as a function of logarithm (to the base of 10) of E. Results clearly show that the patterns are the same for ^{6}Li and ^{7}Li colliding with ^{85}Rb$^+$, but they differ in magnitude, particularly in the low-energy regime. Figure 6 exhibits the variation of s- and p-wave scattering cross sections against energy in log–log scale for both isotopes of Li colliding with Rb$^+$. Again, the results are qualitatively similar for both the isotopes, but they differ slightly quantitatively. Comparing the upper and lower panels in figure 6, one can notice that the Wigner threshold law regime for ^{6}Li can be attained at slightly higher energy than that for ^{7}Li.

4. Conclusions

In conclusion, we have studied elastic scattering between an alkali ion and alkali atom of different nuclei of three ion-atom systems, namely, Li + Cs$^+$, Na + Cs$^+$, and Li + Rb$^+$. We have calculated the interaction potentials and spectroscopic constants of these systems. We have presented a detailed study of elastic collision physics over a wide range of energies, showing the onset of Wigner threshold regime at ultra-low energy and the $1/3$ law of scattering at higher energy regime. The low-energy scattering results presented here may be useful for future exploration for radiative- or photo-associative formation of cold diatomic molecular ions from these three ion-atom systems. The colliding ground state atom-ion pair corresponding to the continuum of $1^2\Sigma^+$ may be photo-associated to form a bound state in second excited potential $3^2\Sigma^+$ by using a laser of appropriate frequency. This is promising because the transition is dipole-allowed and similar to atomic transition. The formation of such cold molecular ions by radiative processes will offer new directions in ultracold chemistry.

Acknowledgments

This work is jointly supported by Department of Science and Technology (DST), Ministry of Science and Technology, Government of India and Ministry of Higher Education and Scientific Research (MHESR), Government of Tunisia, under an India-Tunisia Project for Bilateral Scientific Cooperation.

References

[1] Grier A T, Certina M, Orucevic F and Vuletic V 2009 *Phys. Rev. Lett.* **102** 223201
[2] Hall F H J, Aymar M, Bouloufa N, Dulieu O and Willitsch S 2011 *Phys. Rev. Lett.* **107** 243202
[3] Hall F H J, Eberle P, Hegi G, Raoult M, Aymar M, Dulieu O and Willitsch S 2013 *Mol. Phys.* **111** 2020
[4] Rellergert W, Sullivan S, Kotochigova S, Petrov A, Chen K, Schowalter S and Hudson E 2011 *Phys. Rev. Lett.* **107** 243201
[5] Sullivan S, Rellergert W, Kotochigova S and Hudson E 2012 *Phys. Rev. Lett.* **109** 223002
[6] Zipkes C, Palzer S, Sias C and Kohll M 2010 *Nature* **464** 388
[7] Zipkes C, Palzer S, Ratschbacher L, Sias C and Kohll M 2010 *Phys. Rev. Lett.* **105** 133201
[8] Ratschbacher L, Zipkes C, Sias C and Kohll M 2013 *Nat. Phys.* **8** 649
[9] Haze S, Hata A, Fujinaga M and Mukaiyama T 2013 *Phys. Rev.* A **87** 052715
[10] Schmid S, Härter A, Frisch A, Hoinka S and Hecker-Denschlag J 2012 *Rev. Sci. Instrum.* **83** 053108
[11] Haerter A, Kruekow A, Brunner A, Schnitzler W, Schmid S and Denschlag J H 2012 *Phys. Rev. Lett.* **109** 123201
[12] Sivarajah I, Goodman D S, Wells J E, Narducci F A and Smith W W 2012 *Phys. Rev.* A **86** 063419
[13] Schmid S, Härter A and Denschlag J H 2010 *Phys. Rev. Lett.* **105** 133202
[14] Ravi K, Lee S, Sharma A, Werth G and Rangwala S 2012 *Appl. Phys.* B **107** 971
[15] Ravi K, Lee S, Sharma A, Werth G and Rangwala S 2012 *Nat. Comm.* **3** 2253
[16] Lee S, Ravi K and Rangwala S 2013 *Phys. Rev.* A **87** 052701
[17] Smith W W, Marakov O P and Lin J 2005 *J. Mod. Opts.* **52** 2253
[18] Bissbort U, Cocks D, Negretti A, Idziaszek Z, Calarco T, Schmidt-Kaler F, Hofstetter W and Gerritsma R 2013 *Phys. Rev. Lett.* **111** 080501
[19] Gerritsma R, Negretti A, Doerk H, Idziaszek Z, Calarco T and Schmidt-Kaler F 2012 *Phys. Rev. Lett.* **109** 080402
[20] Joger J, Negretti A and Gerritsma R 2014 *Phys. Rev.* A **89** 063621
[21] Goold J, Doerk H, Idziaszek Z, Calarco T and Busch T 2010 *Phys. Rev.* A **81** 041601
[22] Côté R 2000 *Phys. Rev. Lett.* **85** 5316
[23] Silva H da Jr, Raoult M, Aymar M and Dulieu O 2015 *New J. Phys.* 17
[24] Côté R, Kharchenko V and Lukin M D 2002 *Phys. Rev. Lett.* **89** 093001
[25] Rakshit A and Deb B 2011 *Phys. Rev.* A **83** 022703
[26] Aymar M, Guerout R and Dulieu O 2011 *J. Chem. Phys.* **135** 064305
[27] Tomza M, Koch C P and Moszynski R 2015 *Phys. Rev.* A **91** 042706
[28] Goodman D S, Wells D S, Kwolek J E, Blumel J M, Narducci R and Smith W W F A 2015 *Phys. Rev.* A **91** 012709
[29] Bodo E, Zhang P and Dalgarno A 2008 *New J. Phys.* **10** 033024
[30] Zhang P, Bodo E and Dalgarno A 2009 *J. Phys. Chem.* A **113** 15085
[31] Zygelman B, Dalgarno A, Kimura M and Lane N F 1989 *Phys. Rev.* A **40** 2340
[32] Idziaszek Z, Calarco T, Julienne P S and Simoni A 2009 *Phys. Rev.* A **79** 010702(R)
[33] Gao B 2010 *Phys. Rev. Lett.* **104** 213201
[34] Li M and Gao B 2012 *Phys. Rev.* A **86** 012707
[35] Doerk-Bendig H, Idziaszek Z and Calarco T 2010 *Phys. Rev.* A **81** 012708
[36] Harter A and Denschlag J H 2014 *Contemporary Phys.* **55** 33
[37] Tacconi M, Gianturco F A and Belyaev A K 2011 *Phys. Chem. Chem. Phys.* **13** 19156
[38] Sayfutyarova E R, Buchachenko A A, Yakovleva S A and Belyaev A K 2013 *Phys. Rev.* A **87** 052717
[39] McLaughlin B M, Lamb H D L, Lane T C and McCann J F 2014 *J. Phys. B.: At. Mol. Opt. Phys.* **47** 145201
[40] Zygelman B, Zelimir L and Hudson E R 2014 *J. Phys. B: At. Molec. Opt. Phys.* **47** 015301
[41] Lamb H, McCann J, McLaughlin B, Goold J, Wells N and Lane I 2012 *Phys. Rev.* A **86** 022716
[42] Huber T, Lambrecht A, Schmidt J, Karpa L and Schaetz T 2014 *Nature* **5** 5587
[43] Cooley J W 1961 *Math Comp.* **15** 363
[44] Barthelat J C and Durand Ph 1975 *Theor Chem. Acta* **38** 283
[45] Ghanmi C, Farjallah M and Berriche H 2012 *J. Mol. Spect.* **235** 158
[46] Ghanmi C, Bouzouita H, Berriche H and Ben Ouada H 2006 *J. Mol. STruct. THEOCHEM* **777** 81
[47] Ghanmi C, Farjallah M and Berriche H 2012 *Int. J. Quant. Chem.* **112** 2403
[48] Berriche H 2003 *J. Mol. Struct. THEOCHEM* **663** 101
[49] Berriche H, Ghanmi C and Ben Ouada H 2005 *J. Mol. Spect.* **230** 161
[50] Valance A 1978 *J. Chem. Phys.* **69** 355
[51] Muller W, Flesh J and Meyer W 1984 *J. Chem. Phys.* **80** 3297
[52] Foucrault M, Millie Ph and Daudey J P 1992 *J. Chem. Phys.* **96** 1257
[53] Pavolini D, Gustavsson T, Spiegelmann F and Daudey J P 1989 *J. Phys. B At. Mol. Opt. Phys.* **22** 1721
[54] Bellomonte L, Cavaliere P and Ferrante G 1974 *J. Chem. Phys.* **61** 3225
[55] Carlson N W, Taylor A J and Shawlow A L 1980 *Phys. Rev. Lett.* **45** 18
[56] Patil S H and Tang K T 2000 *J. Chem. Phys.* **113** 676
[57] Azizi S, Aymar M and Dulieu O 2007 *AIP. Conf. Proc.* **935** 164
[58] Khelifi N, Dardouri R and Al-Dossary O M 2011 *J. Appl. Spect.* **78** 11
[59] Press W H, Teukolsky S A, Vetterling W T and Flannery B P 2007 *Numerical Recipes in FORTRAN: The Art of Scientific Computing* 3rd edn (New York: Cambridge University Press)